

TRACKING AIRBORNE TARGETS HIDDEN IN BLIND DOPPLER USING CURRENT STATISTICAL MODEL PARTICLE FILTER

Z. G. Shi, S. H. Hong, and K. S. Chen

Department of Information and Electronic Engineering
Zhejiang University
Hangzhou 310027, China

Abstract—This paper aims at finding an algorithm featuring good estimation performance and easy hardware implementation for tracking airborne target hidden in blind Doppler. Incorporating the current statistical model which is effective in dealing with the maneuvering motions that most blind Doppler issues are caused, a current statistical model particle filter (CSM-PF) is presented in this paper for tracking airborne targets hidden in blind Doppler. Simulation results demonstrate that the proposed CSM-PF shows similar performance with the interacting multiple model particle filter (IMM-PF) in terms of tracking accuracy and track continuity, but it avoids the difficulty of model selection for maneuvering targets. In addition, when hardware implementation is considered, the proposed CSM-PF has lower processing latency, fewer resource utilization and lower hardware complexity than the IMM-PF.

1. INTRODUCTION

Radar systems extract information pertaining to location or velocity of a target upon receiving the measurements. During these years, multifarious new techniques are continuously applied to various radar systems [1–8]. Nowadays, modern radar systems have been regarded to be very “mature” in all the aspects like performance, manufacturing technics and reliability, and have been widely applied in both military and civil uses. However, the development of radar is far from its end. The coming forth of the “electric war” raised new requirements to all aspects of radar systems, such as devices manufacturing, circuit implementation, antenna design and signal processing of radar tracking [9–17]. Among various radar tracking problems, tracking the

targets hidden in radar blind Doppler zone (BDZ) becomes a hot topic in recent years due to its importance in airborne radars [18–20].

Blind Doppler refers to the bands of Doppler frequency where the targets are invisible due to rejection of ground clutter from the radar echoes. In airborne tracking, the blind Doppler makes the target undetectable, resulting in tracking difficulties. Since the target cannot always be hidden in the BDZ and it has to reappear finally, it is highly required that tracking should be resumed as soon as the radar detects the target again. The extended Kalman filter (EKF) and its versatile variations [21] are the most popular approaches for target tracking. However, due to the blind Doppler's severe nonlinearity, the estimation performances of EKF-based methods are not very satisfactory [18]. Preferred means are particle filters (PFs) [22–26] and combined EKF/PFs, which can resume tracking after reappearance of the target by using the prior knowledge of BDZ [18, 19].

Most blind Doppler issues arise from maneuvering motion, and different maneuvering motions will result in different BDZs. For such maneuverabilities, the particle filter based on constant velocity (CV) motion model may have difficulties [18]. Ref. [20] proposed an IMM-PF which combines a constant velocity model and an acceleration model to handle the maneuvering motions. However, the actual models of a target are unknown for the tracking filter, thus the selection of multiple models is very difficult. If the combined models are not selected appropriately, the estimation error will be unacceptable. Further more, the IMM algorithm features high processing latency and complex hardware implementation [20].

Current statistical model is essentially a Signer model with an adaptive mean [27]. It doesn't require any *a priori* model for the diverse acceleration situations of actual target maneuvers. Thus, the difficulty of selecting appropriate models for different maneuvering motions can be avoided. In addition, for tracking maneuvering targets, the current statistical model has fast processing rate and high estimate precision, along with the characteristic of easy hardware implementation. In this paper, we combine the current statistical model and particle filter to built a CSM-PF algorithm to track the targets hidden in blind Doppler.

The layout of this paper is as follows. In Section 2, the problem of tracking airborne targets hidden in blind Doppler is formulated. In Section 3, we briefly outline the current statistical model and present the CSM-PF algorithm for tracking airborne targets hidden in blind Doppler. Simulation results and discussions are given in Section 4 and we conclude this paper in Section 5.

2. PROBLEM FORMULATION

For the airborne target-tracking problem, the target moves within the x - y plane according to the standard model [28]:

$$\mathbf{x}_{k+1} = \mathbf{F}_k \mathbf{x}_k + \mathbf{E}_k \mathbf{u}_k + \mathbf{\Gamma}_k \mathbf{v}_k \quad (1)$$

where $\mathbf{F}_k = \begin{pmatrix} 1 & T & 0 & 0 \\ 0 & 1 & 0 & 0 \\ 0 & 0 & 1 & T \\ 0 & 0 & 0 & 1 \end{pmatrix}$ is the state transition matrix (T

is the sampling interval), $\mathbf{x}_k = [x_k, \dot{x}_k, y_k, \dot{y}_k]'$ is the target state

vector at time kT (k is the time index), $\mathbf{E}_k = \begin{pmatrix} T^2/2 & 0 \\ T & 0 \\ 0 & T^2/2 \\ 0 & T \end{pmatrix}$

and $\mathbf{\Gamma}_k = \begin{pmatrix} T^2/2 & 0 \\ T & 0 \\ 0 & T^2/2 \\ 0 & T \end{pmatrix}$ are the input matrix, $\mathbf{u}_k = [u_k^x, u_k^y]'$ is

the acceleration input vector ($\mathbf{u}_k = 0$ for CV motion model), and $\mathbf{v}_k = [v_k^x, v_k^y]'$ is the vector of input white noise with zero mean. The variables (x_k, y_k) and (\dot{x}_k, \dot{y}_k) in the target state vector \mathbf{x}_k represent the target positions and speeds in the x and y directions, respectively.

The measurement equation is

$$\mathbf{z}_k = h(\mathbf{x}_k) + w_k \quad (2)$$

where $\mathbf{z}_k = [x_k, y_k, \dot{r}_k]'$ consists of position and range-rate measurements. The unbiased conversions of measurements from polar coordinate to Cartesian coordinate are given by: $x_k = \lambda^{-1} \cdot r_k \cdot \cos \theta_k$, $y_k = \lambda^{-1} \cdot r_k \cdot \sin \theta_k$ with $\lambda = \exp(-\sigma_\theta^2/2)$ being the bias compensation factor, r_k and θ_k being the range and the bearing of the target. The error statistics for radar measurements are given in terms of the range standard deviation σ_r , range-rate standard deviation $\sigma_{\dot{r}}$, and azimuth standard deviation σ_θ . With these statistics, the position variances in the respective directions and their cross-covariance are as follows [29]:

$$\sigma_{x_k}^2 = (\lambda^{-2} - 2) r_k^2 \cos^2 \theta_k + (r_k^2 + \sigma_r^2) (1 + \lambda^4 \cos 2\theta_k) / 2 \quad (3)$$

$$\sigma_{y_k}^2 = (\lambda^{-2} - 2) r_k^2 \sin^2 \theta_k + (r_k^2 + \sigma_r^2) (1 - \lambda^4 \cos 2\theta_k) / 2 \quad (4)$$

$$\sigma_{x_k y_k}^2 = (\lambda^{-2} - 2) r_k^2 \cos \theta_k \sin \theta_k + (r_k^2 + \sigma_r^2) \lambda^4 \sin 2\theta_k / 2 \quad (5)$$

The nonlinear function $h(\mathbf{x}_k)$ is defined as:

$$h(\mathbf{x}_k) = \begin{bmatrix} x_k \\ y_k \\ \frac{x_k \dot{x}_k + y_k \dot{y}_k}{\sqrt{x_k^2 + y_k^2}} \end{bmatrix} = \begin{bmatrix} \mathbf{x}_k(1) \\ \mathbf{x}_k(3) \\ \frac{\mathbf{x}_k(1)\mathbf{x}_k(2) + \mathbf{x}_k(3)\mathbf{x}_k(4)}{\sqrt{\mathbf{x}_k^2(1) + \mathbf{x}_k^2(3)}} \end{bmatrix} \quad (6)$$

where $\mathbf{x}_k(i)$ denotes the i th component of the state vector. The measurement noise w_k is a 3×1 zero-mean Gaussian noise vector with covariance matrix:

$$R_k = \begin{bmatrix} \sigma_{x_k}^2 & \sigma_{x_k y_k}^2 & 0 \\ \sigma_{x_k y_k}^2 & \sigma_{y_k}^2 & 0 \\ 0 & 0 & \sigma_{\dot{r}}^2 \end{bmatrix} \quad (7)$$

The process noise v_k and the measurement noise w_k are assumed to be independent. The detection probability according to this model is:

$$P_D(\mathbf{x}_k) = \begin{cases} P_d, & \text{if } \left| \frac{x_k \dot{x}_k + y_k \dot{y}_k}{\sqrt{x_k^2 + y_k^2}} \right| \geq L_0 \\ 0, & \text{otherwise} \end{cases} \quad (8)$$

where L_0 is the limit of BDZ when the platform motion has been compensated and P_d is a positive constant less than or equal to unity.

3. CSM-PF

In this section, we briefly review the current statistical model and present the CSM-PF algorithm for tracking the target hidden in BDZ.

3.1. Current Statistical Model

Current statistical model is essentially a Singer model with an adaptive mean. The current probability density of a target's maneuvering acceleration has the form of modified Raleigh density. The discrete current statistical model is:

$$\mathbf{X}(k+1) = \Phi(k+1, k)\mathbf{X}(k) + \mathbf{U}(k)\bar{\mathbf{a}} + \mathbf{W}(k) \quad (9)$$

where $\mathbf{X}(k) = [x(k) \dot{x}(k) \ddot{x}(k) y(k) \dot{y}(k) \ddot{y}(k)]'$ is a six-dimensional state vector with entries of position, velocity and acceleration, $\bar{\mathbf{a}} = [\bar{a}_x \bar{a}_y]'$

is the mean of current maneuvering acceleration in the Cartesian coordinated x and y .

$$\Phi(k+1, k) = \begin{bmatrix} \mathbf{F}_{k+1/k} & \mathbf{O}_{3 \times 3} \\ \mathbf{O}_{3 \times 3} & \mathbf{F}_{k+1/k} \end{bmatrix} \quad (10)$$

where $\mathbf{F}_{k+1/k} = \begin{bmatrix} 1 & T & (\tau T - 1 + e^{-\tau T})/\tau^2 \\ 0 & 1 & (1 - e^{-\tau T})/\tau \\ 0 & 0 & e^{-\tau T} \end{bmatrix}$, $\mathbf{O}_{3 \times 3}$ is a 3×3 zero matrix and τ is the reciprocal of maneuvering time constant.

$$\mathbf{U}(k) = \begin{bmatrix} \mathbf{U}_1(k) & \mathbf{O}_{3 \times 1} \\ \mathbf{O}_{3 \times 1} & \mathbf{U}_1(k) \end{bmatrix} \quad (11)$$

where $\mathbf{U}_1(k) = [u_{11} \ u_{12} \ u_{13}]'$, $\mathbf{O}_{3 \times 1}$ is a 3×1 zero vector, and $u_{11} = (-\tau T + \tau^2 T^2/2 + 1 - e^{-\tau T})/\tau^2$, $u_{12} = (\tau T - 1 + e^{-\tau T})/\tau$, $u_{13} = 1 - e^{-\tau T}$.

The term $\mathbf{W}(k)$ in Equation (9) is a discrete white process noise and its covariance is

$$\mathbf{Q}(k) = E[\mathbf{W}(k)\mathbf{W}^T(k)] = \begin{bmatrix} \mathbf{Q}_1(k) & \mathbf{O}_{3 \times 3} \\ \mathbf{O}_{3 \times 3} & \mathbf{Q}_1(k) \end{bmatrix} \quad (12)$$

where $\mathbf{Q}_1(k) = 2\tau\sigma_a^2 \begin{bmatrix} q_{11} & q_{12} & q_{13} \\ q_{12} & q_{22} & q_{23} \\ q_{13} & q_{23} & q_{33} \end{bmatrix}$ with

$$q_{11} = (1 - e^{-2\tau T} + 2\tau T + 2\tau^3 T^3/3 - 2\tau^2 T^2 - 4\tau T e^{-\tau T})/(2\tau^5)$$

$$q_{12} = (e^{-2\tau T} + 1 - 2e^{-\tau T} + 2\tau T e^{-\tau T} - 2\tau T + \tau^2 T^2)/(2\tau^4)$$

$$q_{13} = (1 - e^{-2\tau T} - 2\tau T e^{-\tau T})/(2\tau^3)$$

$$q_{22} = (4e^{-\tau T} - 3 - e^{-2\tau T} + 2\tau T)/(2\tau^3)$$

$$q_{23} = (e^{-2\tau T} + 1 - 2e^{-\tau T})/(2\tau^2)$$

$$q_{33} = (1 - e^{-2\tau T})/(2\tau)$$

and σ_a^2 being the variance of current acceleration that can be calculated from the following equation:

$$\sigma_a^2 = \begin{cases} \left(\frac{4 - \pi}{\pi} (a_{max} - \dot{a}(k/k)) \right)^2, & \dot{a}(k/k) > 0 \\ \left(\frac{4 - \pi}{\pi} (a_{-max} - \dot{a}(k/k)) \right)^2, & \dot{a}(k/k) < 0 \end{cases} \quad (13)$$

where $\dot{a}(k/k)$ is the current predicted acceleration, a_{max} and a_{-max} denote the positive and negative boundary value of acceleration.

To avoid the adverse influence of the limited acceleration presupposed in the target tracking, we utilizes the functional relation between the maneuvering status of target and the estimation of the neighboring inter-sample position information to carry out the self-adaptation of the process noise variance:

$$\sigma_a^2 = \frac{4 - \pi}{\pi} \left[\bar{a} + \frac{2}{T^2} \Delta d \right]^2 \quad (14)$$

3.2. CSM-PF Algorithm

The unrestricted sample set is denoted as $\{x_k^U(i) : i = 1, \dots, N_U\}$ and the BDZ set is $\{x_k^{BZ}(i) : i = 1, \dots, N_{BZ}\}$. The overall probability weights attached to each set is denoted as $p_k(U)$ and $p_k(BZ)$. The CSM-PF algorithm is described as follows.

-
- **Initialization:** $k = 1$
 - For $i = 1, \dots, N_U$, sample $\tilde{\mathbf{x}}_1^U(i)$ from $p(\mathbf{x}_1)$
 - Set $p_1(U) = 1$ and $p_1(BZ) = 0$
 - For $k = 2, 3, \dots$
 - **Prediction:**
 - For $i = 1, \dots, N_U$, sample $\tilde{\mathbf{x}}_k^U(i) \sim p(\mathbf{x}_k | \mathbf{x}_{k-1}^U(i))$
 - if $p_{k-1}(BZ) > 0$, for $i = 1, \dots, N_{BZ}$, sample $\tilde{\mathbf{x}}_k^{BZ} \sim p(\mathbf{x}_k | \mathbf{x}_{k-1}^{BZ}(i))$
 - **Information update:**
 - case (1):
 - if $P_d > 0$ and $p_{k-1}(BZ) = 0$, this means the target is detected now and was in unrestricted area in the previous sample time.
 - * Set $p_1(U) = 1$, $p_1(BZ) = 0$
 - * probability weights: $w_k^U(i) \propto p(\mathbf{z}_k | \tilde{\mathbf{x}}_k^U(i))$ to $\tilde{\mathbf{x}}_k^U(i)$
 - * Normalized weights: $w_k^U(i) = w_k^U(i) / \sum_{i=1}^N w_k^U(i)$
 - case (2):
 - if $P_d = 0$ and $p_{k-1}(BZ) = 0$, this means the target is in blind area now but was in unrestricted area in the previous sample time.
 - * Use auxiliary sequential importance sampling [30] to generate $\{\tilde{\mathbf{x}}_k^{BZ}(i)\}$ from $\{\mathbf{x}_{k-1}^U(i)\}$
 - * Assign sample weight: $w_k^{BZ}(i) = N_{BZ}^{(-1)}$ to $\tilde{\mathbf{x}}_k^{BZ}(i)$
 - * Set $p_k(BZ) = P_d$ and $p_k(U) = 1 - P_d$
 - case (3):
 - if $P_d = 0$ and $p_{k-1}(BZ) = 1$, this means the target is in blind

area now and was in blind area in the previous sample time.
(assuming only CV motions in blind zone).

- * Assign sample weight: $w_k^{BZ}(i) = N_{BZ}^{(-1)}$ to $\tilde{\mathbf{x}}_k^{BZ}(i)$
- * Assign sample weight: $w_k^U(i) = N_U^{(-1)}$ to $\tilde{\mathbf{x}}_k^U(i)$
- * Set $p_k(U) = (1 - P_d)p_{k-1}(U)$ and $p_k(BZ) = 1 - p_k(U)$

– case (4):

if $P_d > 0$ and $p_{k-1}(BZ) = 1$, this means the target is detected but was in blind area in the previous sample time.

- * Generate $\mathbf{x}_k^U(i)$ by selecting the larger one from $\{\tilde{\mathbf{x}}_k^U(i)\}$ and $\{\tilde{\mathbf{x}}_k^{BZ}(i)\}$.
- * Probability weights: $w_k^U(i) \propto p(\mathbf{z}_k | \mathbf{x}_k^U(i))$
- * Normalized weights: $w_k^U(i) = w_k^U(i) / \sum_{i=1}^N w_k^U(i)$
- * Set $p_1(U) = 1, p_1(BZ) = 0$

- **Resampling and roughening**

- Multiply or discard particles with respect to high or low normalized importance weights to obtain N_U particles $\{\mathbf{x}_k^U(i)\}$ and N_{BZ} particles $\{\mathbf{x}_k^{BZ}(i)\}$.
- Roughen the particles after resampling to improve the diversity among particles using the typical roughening method [31].

- **Output**

- Output the weighted mean $\bar{\mathbf{x}}_k = p_k(U) \sum_{i=1}^{N_U} w_k^U(i) \mathbf{x}_k^U(i) + p_k(BZ) \sum_{i=1}^{N_{BZ}} w_k^{BZ}(i) \mathbf{x}_k^{BZ}(i)$

- **Update the variance of current acceleration σ_a^2**

–

$$\sigma_{a_x}^2 = \frac{4 - \pi}{\pi} \left[\bar{a}_x + \frac{2}{T^2} (\bar{\mathbf{x}}_k(1) - \bar{\mathbf{x}}_{k-1}(1) - \bar{\mathbf{x}}_{k-1}(2)T - \frac{1}{2} \bar{\mathbf{x}}_{k-1}(3)T^2) \right]^2$$

–

$$\sigma_{a_y}^2 = \frac{4 - \pi}{\pi} \left[\bar{a}_y + \frac{2}{T^2} (\bar{\mathbf{x}}_k(4) - \bar{\mathbf{x}}_{k-1}(4) - \bar{\mathbf{x}}_{k-1}(5)T - \frac{1}{2} \bar{\mathbf{x}}_{k-1}(6)T^2) \right]^2$$

- **Next k**

4. SIMULATION RESULTS AND DISCUSSIONS

In this section, we show the merits of the CSM-PF algorithm when it is applied to tracking airborne targets hidden in DBZs.

4.1. Simulation Results

We evaluated the performance of the proposed CSM-PF algorithm by considering the root-mean square (RMS) position errors and the probability of track maintenance. As in Ref. [18], we introduce the track score S_k to define a track loss, which is computed as follows.

$$S'_k = \begin{cases} S^{k-1} + \delta^+(T_k) & \text{if target detected and } \mathbf{z}_k \text{ gated} \\ S^{k-1} - \delta^+(T_k) & \text{otherwise} \end{cases} \quad (15)$$

$$S_k = \begin{cases} \min(S'_k, 1) & \text{if target detected and } \mathbf{z}_k \text{ gated} \\ \max(S'_k, 0) & \text{otherwise} \end{cases} \quad (16)$$

where the parameters $\delta^+(T_k)$ and $\delta^-(T_k)$ are the score increment and decrement, respectively. When the track score S_k falls below a certain threshold, the track is regarded as lost.

For comparison, the results of tracking targets hidden in blind Doppler using PFs in [18] and the IMM-PF in [20] are presented to gauge the performance. The target trajectory is shown in Fig. 1, which is a typical scenario of interest [20]. Starting with a constant velocity of 800 km/h toward the radar for 30 seconds, the target makes a $3g$ ($g = 9.81 \text{ m/s}^2$ is gravity acceleration) turn to its right and continues the tangential motion with respect to radar until 45 seconds. Then it makes the second $3g$ turn and flies at the original velocity for 24 seconds. After making the third $3g$ turn to its left, it continues the tangential motion for 10 seconds. Finally, the target makes another $3g$ turn to the right and moves at the original velocity. In the whole flight, the target intends to make two BDZs as indicated in Fig. 1. The time evolution of target range-rate is shown in Fig. 2 together with the limit L_0 of BDZs.

In simulations, the parameters are as follows: The sampling interval is $T = 1 \text{ s}$; the process noises are $\sigma_{v_x} = \sigma_{v_y} = 3 \text{ m/s}$; the error statistics for radar measurements are $\sigma_r = 30 \text{ m/s}$, $\sigma_{\dot{r}} = 3 \text{ m/s}$, and $\sigma_\theta = 0.3 \text{ rad}$; the limit of BDZ is $L_0 = 30 \text{ m/s}$; the detection probability is $P_d = 0.9$; the gating probability is $P_g = 0.995$; the track score parameters are $\delta^+(T_k) = 0.02$ and $\delta^-(T_k) = 0.02$. We set $N_U = N_{BZ} = 3000$ for the PF in [18], the CSM-PF and each selected model of the IMM-PF in [20]. For the current statistical model, the reciprocal of maneuvering time constant is $\tau = 0.02$.

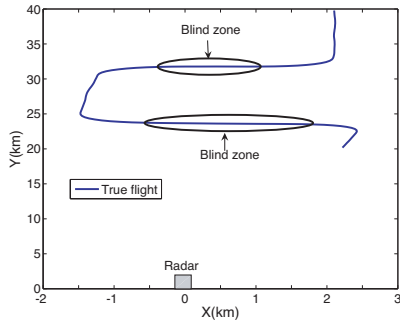


Figure 1. A typical tracking scenario of interest.

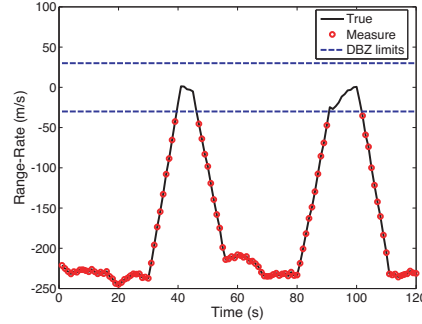


Figure 2. Range-rate of the typical tracking flight.

Figure 3 shows the RMS position errors. As in [24], the RMS position error at time index k is defined as:

$$RMS_k = \sqrt{\frac{1}{M} \sum_{i=1}^M (\hat{x}_k^i - x_k^i)^2 + (\hat{y}_k^i - y_k^i)^2} \quad (17)$$

where $M = 50$ is the Monte Carlo simulation times, and \hat{x}_k^i, \hat{y}_k^i are the filter position estimations at time index k in i th Monte Carlo simulation. It can be found that the IMM-PF in [20] and the CSM-PF can keep tracking for all the turning sections and thus stayed not far away from the target when the target is about to reappear, but the PF in [18] cannot follow the target from the moment it entered the BDZ and thus failed to resume tracking at the reappearance of the target.

Figure 4 shows that for the track score parameters, the PF in [18] falls down to zero in the middle of the track period, which means that it lost the track. The IMM-PF in [20] and the CSM-PF can maintain a track score not less than 0.6.

4.2. Discussions

From the simulation results above, it can be found that without any information about the actual model of target, the CSM-PF algorithm shows similar performance with the IMM-PF in [20] and both of them show better performance than the PF in [18]. Note here that other than the IMM-PF, the CSM-PF requires no information about the model of target, thus it can avoid the difficulty of model selection for different maneuvering motions. This is a very good characteristic of CSM-PF. In the following part, we will show that the CSM-PF is better than the

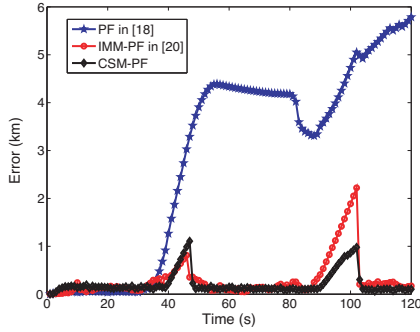


Figure 3. RMS position error versus time for the typical tracking flight.

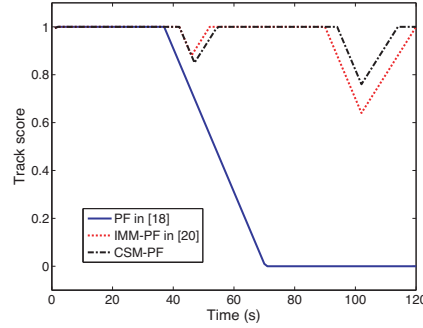


Figure 4. Track score S_k .

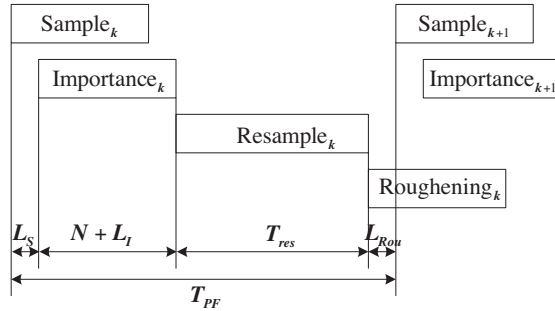


Figure 5. Timing of operations in the case (1) in CSM-PF.

IMM-PF in [20] in terms of processing latency and resource utilization when hardware implementation issues are considered.

For the processing latency, without loss of generality, we only consider the case (1) in the **information update** part of the CSM-PF algorithm where the target is detected and was in unrestricted area in the previous sample time. Fig. 5 shows the timing of operations for one recursion of the CSM-PF. The total cycle time of the CSM-PF is $T_{PF} = (N + L_S + L_I + T_{Res} + L_{Rou})T_{clk}$, where L_S , L_I and L_{Rou} represent the startup latencies of the sample, importance and roughening unit, respectively, T_{Res} is the number of cycles required for resampling, N is the number of particles and T_{clk} is the system clock period. The CSM-PF algorithm requires no additional execution time to estimate the target state and update the variance of current acceleration since it can be processed simultaneously with the resampling unit. When using the compact resampling or the residual systematic resampling [32], the

execution time is $T_{Res} = N + L_{Res}$, where L_{Res} is the latency of the data path. Therefore, the execution time of the CSM-PF is $T_{PF} = (N + L_S + L_I + N + L_{Res} + L_{Rou})T_{clk} = (2N + L_S + L_I + L_{Res} + L_{Rou})T_{clk}$. However, for the IMM-PF, besides the execution time that each selected model requires, it needs additionally interaction stage and combination stage. Thus, the IMM-PF has higher processing latency.

As for resource utilization, taking the IMM-PF in [20] for example, since it combines two different models, it will require roughly twice hardware resources of the proposed CSM-PF. The more models the IMM-PF has, the more resources it requires. Further more, it has to calculate the mixed probabilities and model probabilities, which require expensive operations like divisions. These will result in that the hardware implementation of the IMM-PF has much higher complexity than the proposed CSM-PF.

5. CONCLUSION

In this paper, we have presented a CSM-PF, which is capable of adaptively handling the maneuvering motions, to track airborne targets hidden in blind Doppler. Simulation results demonstrate that the proposed CSM-PF algorithm shows similar performance as the IMM-PF regarding the RMS performance and the probability of track maintenance, but it avoids the difficulty of model selection in IMM-PF for the maneuvering target. Further more, the proposed CSM-PF algorithm has lower processing latency, fewer resource utilization and lower complexity than the IMM-PF when hardware implementation issues are considered.

ACKNOWLEDGMENT

This work was supported by National Natural Science Foundation of China (No. 60531020), Zhejiang Provincial Natural Science Foundation of China (No. Y107285) and Chinese Post-Doctoral Science Foundation (No. 20060400313). The authors wish to thank Dr. H. S. Chen for useful discussions of paper layout.

REFERENCES

1. Garenaux, K., T. Merlet, and M. Alouini, "Recent breakthroughs in RF photonics for radar systems," *IEEE Aerospace and Electronic Systems Magazine*, Vol. 22, No. 2, 3–8, 2007.

2. Chan, Y. K. and S. Y. Lim, "Synthetic aperture radar (SAR) signal generation," *Progress In Electromagnetics Research B*, Vol. 1, 269–290, 2008.
3. Wang, C. J., B. Y. Wen, Z. G. Ma, W. D. Yan, and X. J. Huang, "Measurement of river surface current with FWCW radar system," *Journal of Electromagnetic Waves and Applications*, Vol. 21, No. 3, 375–386, 2007.
4. Narayanan, R. M. and C. Kumru, "Implementation of fully polarimetric random noise radar," *IEEE Antennas and Wireless Propagation Letters*, Vol. 4, 125–128, 2005.
5. Abdelaziz, A. A., "Improving the performance of an antenna array by using radar absorbing cover," *Progress In Electromagnetics Research Letters*, Vol. 1, 129–138, 2008.
6. Wang, X., X. Guan, X. Ma, D. Wang, and Y. Su, "Calculating the poles of complex radar targets," *Journal of Electromagnetic Waves and Applications*, Vol. 20, No. 14, 2065–2076, 2006.
7. Shi, Z. G., S. Qiao, K. S. Chen, W. Z. Cui, W. Ma, T. Jiang, and L. X. Ran, "Ambiguity functions of direct chaotic radar employing microwave chaotic Colpitts oscillator," *Progress In Electromagnetics Research*, PIER 77, 1–14, 2007.
8. Hebeish. A. A., M. A. Elgamel, R. A. Abdelhady, and A. A. Abdelaziz, "Factors affecting the performance of the radar absorbant textile materials of different types and structus," *Progress In Electromagnetics Research B*, Vol. 3, 219–226, 2008.
9. Liu, H. W., T. Yoshimasu, and L. L. Sun, "CPW bandstop filter using periodically loaded slot resonators," *Electronics Letters*, Vol. 42, No. 6, 352–353, 2006.
10. Ghosh, S. and A. Chakrabarty, "Estimation of equivalent circuit of loaded trans-receive antenna system and its time domain studies," *Journal of Electromagnetic Waves and Applications*, Vol. 20, No. 1, 89–103, 2006.
11. Mahanti, R. G. K., A. Chakrabarty, and S. Das, "Design of fully digital controlled reconfigurable array antennas with fixed dynamic range," *Journal of Electromagnetic Waves and Applications*, Vol. 21, No. 1, 97–106, 2007.
12. Capineri, L., D. Daniels, P. Falorni, O. Lopera, and C. Windsor, "Estimation of relative permittivity of shallow soils by using the ground penetrating radar response from different buried targets," *Progress In Electromagnetics Research Letters*, Vol. 2, 63–71, 2008.

13. Prasad, N. N. S. S. R. K., V. Shameem, U. B. Desai, and S. N. Merchant, "Improvement in target detection performance of pulse coded Doppler radar based on multicarrier modulation with fast Fourier transform (FFT)," *IEE Proceedings - Radar, Sonar and Navigation*, Vol. 151, No. 1, 11–17, 2004.
14. Xue, W. and X. W. Sun, "Target detection of vehicle volume detecting radar based on Wigner-Hough transform," *Journal of Electromagnetic Waves and Applications*, Vol. 21, No. 11, 1513–1523, 2007.
15. Rajabi, M., M. Mohammadirad, and N. Komjani, "Simulation of ultra wideband microstrip antenna using EPML-TLM," *Progress In Electromagnetics Research B*, Vol. 2, 115–124, 2008.
16. Liu, H. W., S. Ishikawa, A. An, S. Kurachi, and T. Yoshimasu, "Miniaturized microstrip meander-line antenna with very high-permittivity substrate for sensor applications," *Microwave and Optical Technology Letters*, Vol. 49, No. 10, 2438–2440, 2007.
17. Guo, Y. C., L. Xu, and X. W. Shi, "Improved loading profile for GPR antenna applications," *Journal of Electromagnetic Waves and Applications*, Vol. 21, No. 10, 1367–1378, 2007.
18. Gordon, N. and B. Ristic, "Tracking airborne targets occasionally hidden in the blind Doppler," *Digital Signal Processing*, Vol. 12, 383–393, 2002.
19. Zaugg, D. A., A. A. Samuel, D. E. Waagen, and H. A. Schmitt, "A combined particle/Kalman filter for improved tracking of beam aspect targets," *IEEE Workshop on Statistical Signal Processing*, 535–538, 2003.
20. Du, S. C., Z. G. Shi, W. Zang, and K. S. Chen, "Using interacting multiple model particle filter to track airborne targets hidden in blind Doppler," *Journal of Zhejiang University Science A*, Vol. 8, No. 8, 1277–1282, 2007.
21. Tanizaki, H., *Nonlinear Filters: Estimation and Application*, Springer, Berlin, Germany, 1996.
22. Doucet, A., N. D. Freitas, and N. Gordon, *Sequential Monte Carlo Methods in Practice*, Springer, New York, USA, 2001.
23. Arulampalam, M. S., S. Maskell, N. Gordon, and T. Clapp, "A tutorial on particle filters for online nonlinear/non-Gaussian Bayesian tracking," *IEEE Transaction on Signal Processing*, Vol. 50, No. 2, 174–188, 2002.
24. Ristic, B., S. Arulampalam, and N. Gordon, *Beyond the Kalman Filter: Particle Filter for Tracking Applications*, Artech House, Boston, 2004.

25. Zang, W., Z. G. Shi, S. C. Du, and K. S. Chen, "Novel roughening method for reentry vehicle tracking using particle filter," *Journal of Electromagnetic Waves and Applications*, Vol. 21, No. 14, 1969–1981, 2007.
26. Hong, S. H., Z. G. Shi, and K. S. Chen, "Novel roughening algorithm and hardware architecture for bearings-only tracking using particle filter," *Journal of Electromagnetic Waves and Applications*, Vol. 22, 411–422, 2008.
27. Singer, R. A., "Estimating optimal tracking filter performance for manned maneuvering targets," *IEEE Aerospace and Electronic Systems Magazine*, Vol. 6, No. 4, 473–483, 1970.
28. Li, X. R. and V. P. Jilkov, "Survey of maneuvering target tracking-Part I: dynamic models," *IEEE Aerospace and Electronic Systems Magazine*, Vol. 39, No. 4, 1333–1364, 2003.
29. Mo, L. B., X. Q. Song, Y. Y. Zhou, et al., "Unbiased converted measurements for tracking," *IEEE Transaction on Aerospace and Electronic Systems*, Vol. 34, No. 3, 1023–1027, 1998.
30. Pitt, M. K. and N. Shephard, "Filtering via simulation: auxiliary particle filter," *Journal of the American Statistical Association*, Vol. 94, No. 446, 590–599, 1999.
31. Gordon, N. J., D. J. Salmond, and A. F. M. Smith, "Novel approach to nonlinear/non-Gaussian Bayesian state estimation," *IEE Proceeding-F*, Vol. 140, No. 2, 107–113, 1993.
32. Bolic, M., P. M. Djuric, and S. Hong, "Resampling algorithms for particle filters: A computational complexity perspective," *EURASIP Journal of Applied Signal Processing*, No. 15, 2267–2277, 2004.